The Effect of Zinc Oxide Nanoparticles (ZnONPs) on the Cerebellum of Adult Male Albino Rats and The Possible Protective Role of Selenium and Fucoidan (Histological and Immunohistochemical Study)

Amal G. Metwally [1], Omima R. Mohamed [2], Amina M.Nagah [3], and Nehal F. Shaheen [4]

KEYWORDS
ACE2, Cerebellum, ZnONps, Selenium, Fucoidan.

ABSTRACT

Zinc oxide nanoparticles, have garnered a lot of attention due to their rapidly growing uses in several industries. The aim was to evaluate the impact of ZnONPs on rat cerebellar tissue and the possible neuroprotective function of fucoidan and selenium. fifty adult albino rats were separated into five groups; group I (control); Ia received no treatment, Ib received (IP) injections of normal saline (0.9%), Ic were given filtered water, Group II were given 400 mg/kg b.wt. of ZnONPs intraperitoneally for 1 month, group III were given ZnONPs injections plus selenium orally at a dosage of 0.5 mg/kg b.wt./day for 1 month, group IV were given ZnONPs injections plus an intraperitoneal injection of fucoidan at a daily dose of 80 mg/kg body weight for 1 month and group V were given ZnONPs injections plus selenium and fucoidan for 1 month. The cerebellar cortex specimens were prepared for histological, biochemical, and immunohistochemical investigation. Evaluations were conducted using both morphometric and statistical methods. ZnONPs significantly raised MDA levels, while significantly lowering SOD and GSH levels in comparison to control group. Histologically, Purkinje cells were destroyed. While the average area percent of glial fibrillary acidic protein (GFAP) and caspase-3-positive cells' immunostain substantially increased, the optical density of calcium binding protein (calbindin) immunopositive cells dramatically reduced. In comparison to the ZnONPs group, both selenium and fucoidan treatments significantly reduced MDA levels and significantly improve SOD and GSH levels. So administration of selenium and fucoidan significantly ameliorated the cerebellar alterations induced by ZnONPs in rats.

Introduction

Nanoparticles (NPs) are materials, either natural or manufactured, with a diameter of less than 100 nm**.** Despite their beneficial effects, they can release reactive oxygen species (ROS), which could affect intracellular biomolecules (Torabi et al., 2017).

Zinc oxide nanoparticles (ZnONPs) are found in food additives, toothpaste, sunscreens, wall paints, cosmetics, and building materials. There are several ways for humans to come in contact with ZnONPs. When taken orally, it can reach the brain through the blood brain barrier (BBB) or through the olfactory route (Ibrahim et al., 2016).

Previous studies described that ZnONPs may easily cross the cell membrane then, interact with the macromolecules of cell, they can produce cytotoxic effects as it promotes neuroinflammation, which is caused by

[(1)]Anatomy and Embryology Department, Faculty of Medicine- Benha University, Benha, Egypt.
[(2)]Forensic Medicine and Clinical Toxicology Department, Faculty of Medicine- Benha University, Benha, Egypt.
[(3)]Neurology Department, Faculty of Medicine- Benha University, Benha, Egypt.
[(4)]Anatomy and Embryology Department, Faculty of Medicine- Benha University, Benha, Egypt.
*** Corresponding author:** Omima R. Mohamed
Address: Benha, Egypt.
Telephone: +2 01223027979
Email: omimarefaat1331@gmail.com

proinflammatory cytokines, as well as apoptosis (Attia et al., 2018).

Fucoidan is an edible brown seaweed-derived natural substance that contains alginate and sulfated polysaccharides. It has a neuroprotective, anti-inflammatory, and anticancer effects (Wang et al., 2021).

Selenium is a vital trace element that is required to maintain growth and health due to its potent antioxidant properties (Zhang et al., 2020).

By scavenging reactive oxygen species (ROS), it helps lessen cell damage. Selenium deficiency is said to be linked to illnesses and nervous system necroptosis (Bi et al., 2022).

The current study's objectives are to examine how ZnONPs affect rats' cerebellar and assess any potential protective benefits of fucoidan and selenium.

Materials and Methods

Materials:

Animals:

Fifty fully grown male albino rats weighing between 200 and 250 grams were purchased from the Breeding Animal House at the Faculty of Medicine at Zagazig University in Zagazig, Egypt. They were kept at room temperature in stainless steel cages under standard laboratory settings. They were given water and standard lab food.

Chemicals:

ZnONPs: As a dispersion containing particles that are typically less than 40 nanometers and a weight percentage of 20 wt % in water.

Characterization of ZnONPs: Transmission electron microscopy (TEM, 1010; Jeol Ltd., Tokyo, Japan), which is housed in the Electron Microscope Entity of the Faculty of Agriculture at Mansoura University in Mansoura City, Egypt, was used to size and shape ZnONPs (Figure 1).

Fucoidan: In the form of powder .In order to create a solution of 16 mg/ml, we dissolved 80 mg of fucoidan in 5 milliliters of normal saline.

Selenium: was bought as a 5 gram powder. One milliliter of distilled water was used to dissolve each rat's prescribed dosage.

The Sigma-Aldrich Chemical Company (St. Louis, MA, USA) was the provider of all chemicals.

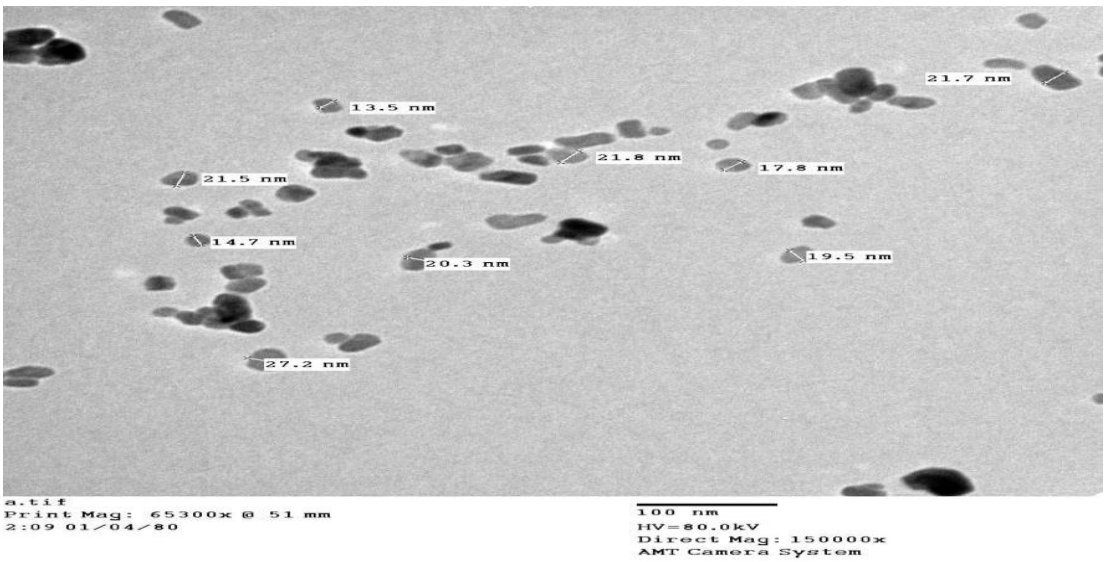

Fig. (**1**): ZnONPs suspension's transmission electron micrograph reveals that the majority of the nanoparticles have a diameter of less than 40 nm.

Study design:

Rats were divided into five groups at random, each consisting of ten animals:

Group I (Control Group): Ten rats were used, and they were split up into three smaller subgroups:

Subgroup Ia: Four rats receive absolutely no treatment.

Subgroup Ib: Three rats received intraperitoneal (IP) injections of normal saline (0.9%).

Subgroup Ic: Using a stomach tube, three rats were given filtered water.

Group II (ZnONPs treated Group): Over the course of a month, 400 mg/kg BW of ZnONPs were intraperitoneally administered into ten rats every other day (Somayeh and Mohammad, 2014)

Group III (ZnONPs + Selenium group): Ten rats received ZnONPs as in group II, and they were also given selenium orally via a gastric tube for a month with a daily dose of 0.5 mg/kg BW (Bekheet, 2020)

Group IV (ZnONPs + fucoidan Group): Ten rats received ZnONPs as in group II, simultaneous with a daily dose of 80 mg/kg BW of fucoidan administered intraperitoneally (Che et al., 2017)

Group V (ZnONPs + Selenium + fucoidan Group): Ten rats received ZnONPs. In addition, selenium was given orally at a dose 0.5 mg/kg BW/day, and fucoidan was given intraperitoneally every day for a month at a dose 80 mg/kg.

Sample Collection:

After a month, the animals were given a chloroform anesthesia. After making a mid-sagittal incision in the skull, the cerebellum was removed. Mid-sagittally, each cerebellum was divided in half, and each portion was preserved at -80° Celsius for biochemical examination. Other portions of the cerebellum tissue were preserved in Bouin's fluid. To prepare the tissues for light microscopy, they were treated.

Biochemical study:

Malondialdehyde (MDA) which is a lipid peroxidation indicator was assessed in cerebellar homogenate (Ohkawa et al., 1979).

The glutathione (GSH) level was verified in cerebellar tissue through Beutler's method (Beutler et al., 1963) additionally, the activity of superoxide dismutase (SOD) was measured as designated by Nishikimi technique (Nishikimi et al., 1972).

All the above kits provided by Bio diagnostic, Cairo, Egypt (Catalog Number: MD 25 29, Catalog Number: GR 25 11, Catalog Number: SD 25 21, correspondingly).

Light microscopic study

- Histological study: Right hemisphere cerebellar tissues were kept in buffered formalin (10%), handled then placed into blocks of paraffin. They were then split at the parasagittal level at a 5μm thickness and thereafter discolored with Hematoxylin and Eosin (H&E) for a standard histology test (Kiernan, 2015).
- Immunohistochemical study:
  a. Glial fibrillary acidic protein (GFAP) for neuroglial astrocyte detection.
  b. Caspase-3 for revealing of apoptosis.
  c. Calcium binding protein (Calbindin)

Avidin Biotin complex technique was utilized for immunohistochemical staining. Specimens encased in paraffin underwent xylene deparaffinization and distilled water hydration. Using citrate buffer, antigen repossession was carried out in the microwave for fifteen minutes. Tissue block was accomplished using bovine serum albumin. After that, the sectors were incubated overnight at 4°C with the following primary antibodies added: anti-caspase-3 antibody (rabbit polyclonal antibody,Lab Vision Thermo Fisher Scientific, USA, cat. number RB-1197-R7), anti-GFAP (Cat. No. MS280- R7, Lab Vision Corporation, Fremont, USA) was diluted to 1:100. Finally, Anti CbD28k (rabbit polyclonal antibody; Cat. No. PA5-85669; dilution 1/500; Thermo Scientific, San Jose, CA, USA) was added. Horseradish peroxidase trailed by colorimetric revelation by 3′, 3-diaminobenzidine (DAB) was characterized by secondary antibodies and appreciated. Mayer's Hematoxylin was used as a counterstain. Phosphate-buffered saline was used to immerse negative control slides (Ramos-Vara et al., 2008).

- Morphometric Study: Morphometric analysis was performed by "ImageJ" software (versoin 1.48v, National Institutes of Health, Bethesda, Maryland, USA). For each slide, 10 picked up at random, non-overlapping fields were studied at 400x magnification to estimate the numeral of Purkinje cells in H&E discolored sections, average area percentage of positive immunohistochemical staining for GFAP, caspase-3 and calbindin D28K positive immunoreactive cells in the immunostained sections.

Ethical consideration: Every experimental procedure followed Official Animal Care and Practice Committee's recommendations and received approval from Benha Faculty of Medicine, Benha University, Egypt, number Rc 25 - 11 -2023.

Statistical analysis

The collected data was analyzed using the statistical package for the social sciences (SPSS) software, version 20 (SPSS Inc., Chicago, Illinois, USA). The P value was considered very significant if it was 0.05. Every data set was displayed as mean ± SD.

Results

Oxidative stress indicators:

According to the indicated data in Table 1, group II exhibited substantial upsurge in the tissue MDA level with concurrent decrease in the tissue GSH and SOD compared with group I (P≤ 0.05). Dissimilar to group II, each of group III as well as group IV presented considerable decrease in the level of MDA and momentous augmentation of SOD and GSH levels (P≤ 0.05). Interestingly, group V noticeably returned all the altered parameters to levels near to that of control animals.

Table (1): Oxidative stress indicators among the studied groups (Mean ±SD)

	Group I (n=10)	Group II (n=10)	Group III (n=10)	Group IV (n=10)	Group V (n=10)	P value
MDA (nmol/g tissue)	1.7 ± 0.08	4.7 ± 0.13	2.5 ± 0.13	2.6 ± 0.12	2.0 ± 0.08	<0.001*
Post-hoc	II,III,IV,V	I,III,IV,V	I,II,V	I,II,V	I,II,III,IV	
GSH (mmol/g tissue)	9.0 ± 0.4	4.4 ± 0.19	7.2 ± 0.19	6.4 ± 0.08	8.5 ± 0.18	<0.001*
Post-hoc	II,III,IV,V	I,III,IV,V	I,II,IV,V	I,II,III,V	I,II,III,IV	
SOD (U/g)	28.8 ±0.23	19.9 ± 0.49	26.3 ± 0.16	25.9 ± 0.21	28.4 ± 0.15	<0.001*
Post-hoc	II,III,IV	I,III,IV,V	I,II,V	I,II,V	II,III,IV	

*: significant as P value ≤ 0.05, MDA: Malondialdehyde, GSH: Glutathione, SOD: Superoxide dismutase.
n: number, SD: standard deviation, nmol: number of moles, mmol:mili mole, U/g: microgram

Histological findings

Slices from the control group showed a molecular layer with basket cells and stellate cells dispersed throughout. The purkinje cell layer was arranged in a single row that had a pyriform appearance, big vesicular nuclei, and visible nucleoli, along with basophilic cytoplasm. Densely packed granule cells with black, round nuclei and an acidophilic cerebellar island were visible in the granular layer (Figure 2).

The structure of the cerebellar tissue was noticeably changed in group II. The molecular layer revealed vacuolated neuropil with multiple pericellular halos. The purkinje cells seemed distorted, disorganized and had irregular shape with dark pyknotic nuclei. The granular cell layer included gaps in between the cellular aggregation (Figure 3).

Sections from group III presented improved histological construction. The purkinje cells seemed as one row of pyriform shaped cells having vesicular nucleus and basophilic cytoplasm. However, some of them had deep stained nuclei. There were also few pericellular spaces (Figure 4).

Group IV exhibited few pericellular spaces in the molecular layer. Some of Purkinje cells had typical appearance with vesicular nucleus and basophilic cytoplasm. Others were irregular in shape and their nuclei were pyknotic (Figure 5).

While, group V displayed relatively normal construction of the cerebellar tissue, there were apparent normal molecular layer and one row of pyriform shaped purkinje cells. Only few of them still showed pyknotic nuclei (Figure 6).

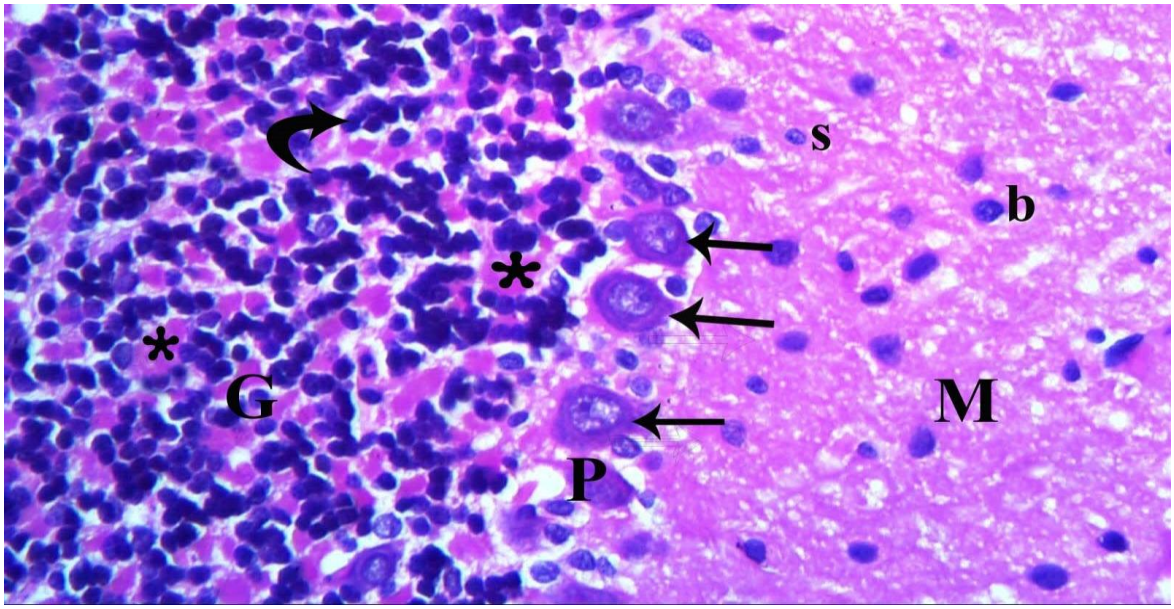

Fig. (2): An H&E-stained photomicrograph of cerebellar sector (**X400**) from group I: Demonstrating the cerebellar cortex three layers; the molecular layer (**M**) contains lightly acidophilic neuropil with large basket cell (**b**), and smaller stellate cell (**s**). Purkinje cells (**P**) layer organized into one row with cytoplasmic basophilia and vesicular nucleus (**arrows**). Granular (**G**) layer contains rounded, small crowded granule cells (**curved arrow**) and acidophilic cerebellar islands (*).

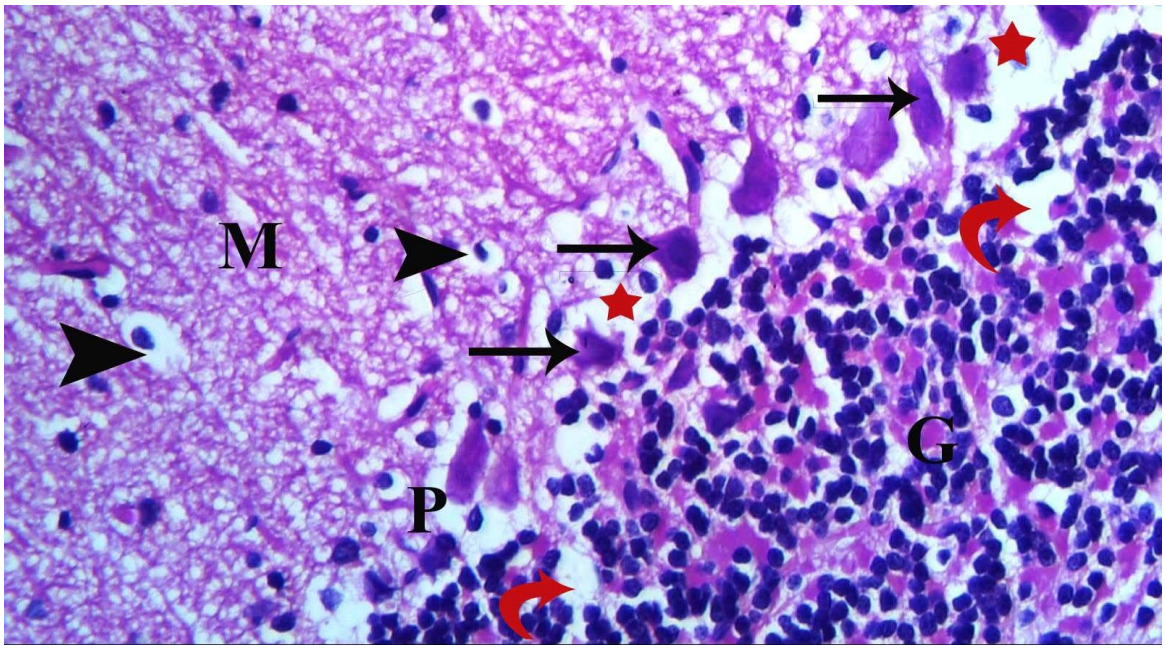

Fig. (3): An H&E-stained photomicrograph of cerebellar sector (**X400**) from of group II: Displaying multiple pericellular halos (**arrow head**). The Purkinje (**P**) cells are distorted, have irregular outline with pyknotic nuclei (**black arrows**), vacuolated neuropil (**stars**) around them. Granular cell (**G**) layer displaying spaces (**curved arrow**) between the granule cells.

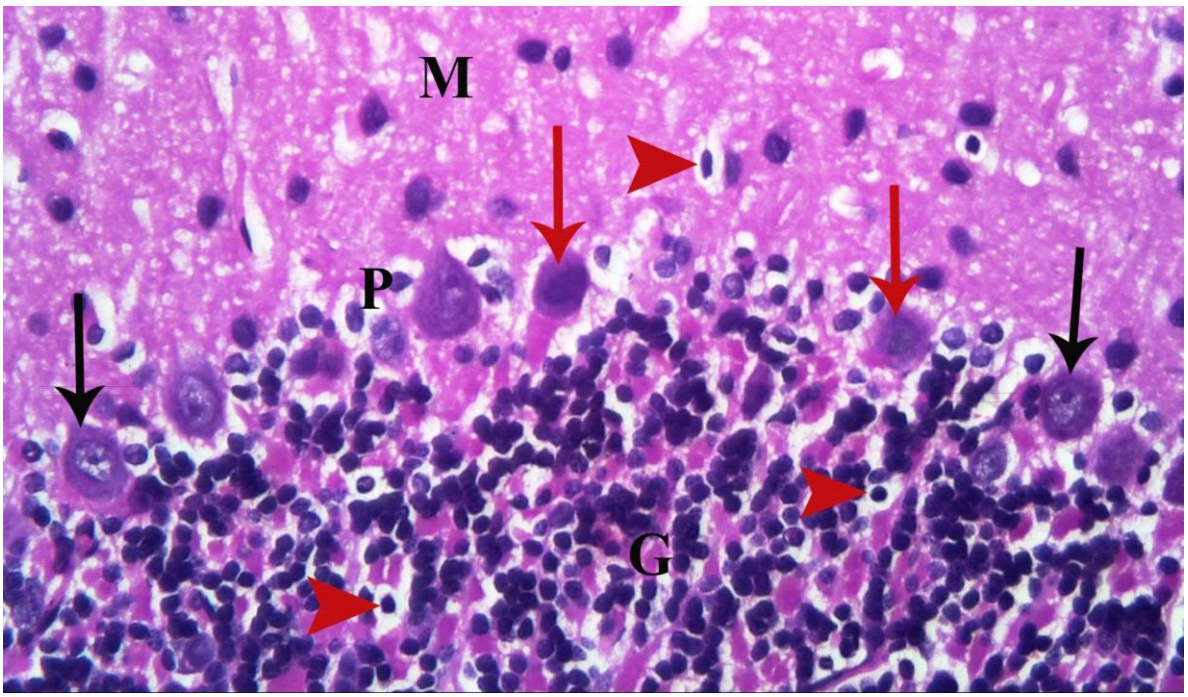

Fig. (4): An H&E-stained photomicrograph of cerebellar slice (**X400**) from group III: Presenting Purkinje cell (**P**) layer appeared as a single row of pyriform cells with cytoplasmic basophilia and vesicular nuclei (**black arrows**). However, some of them have deep stained nuclei (**red arrows**). Notice, few pericellular spaces (**arrow head**) appeared in both the granule cell (**G**) and molecular (**M**) layers.

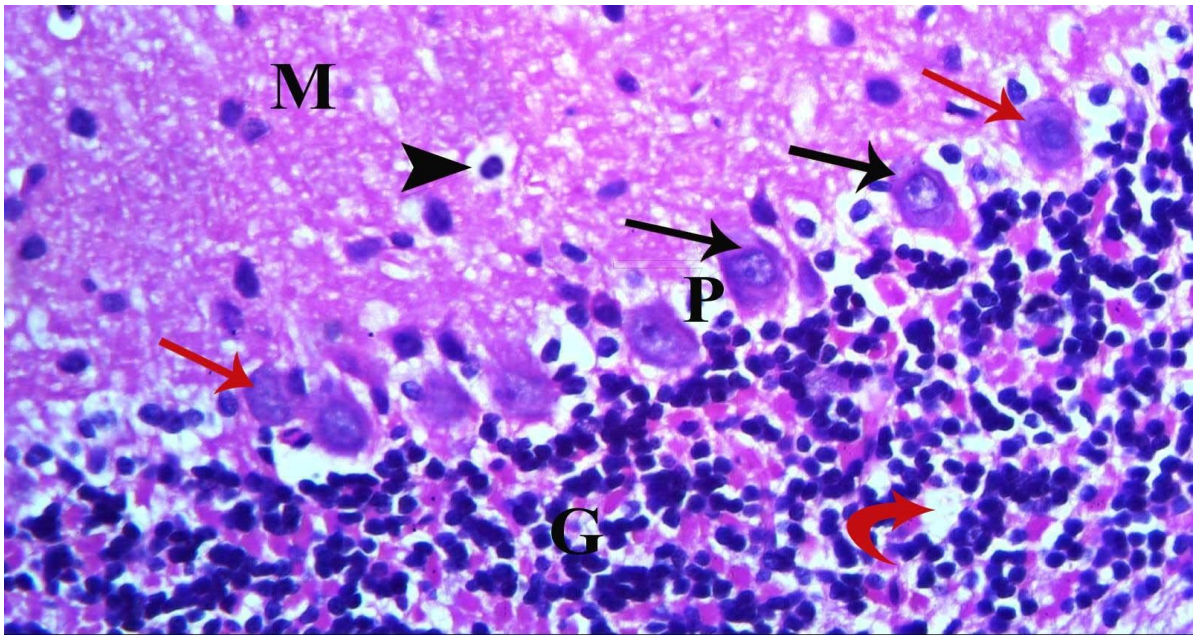

Fig. (5): An H&E-stained photomicrograph of cerebellar sector (**X400**) from group IV: showing few pericellular spaces (**arrow head**) in molecular (**M**) layer. Some of Purkinje cells with normal appearance (**black arrows**). Others (**red arrows**) have pyknotic nuclei. Granular cell (**G**) layer showing space (**curved arrow**).

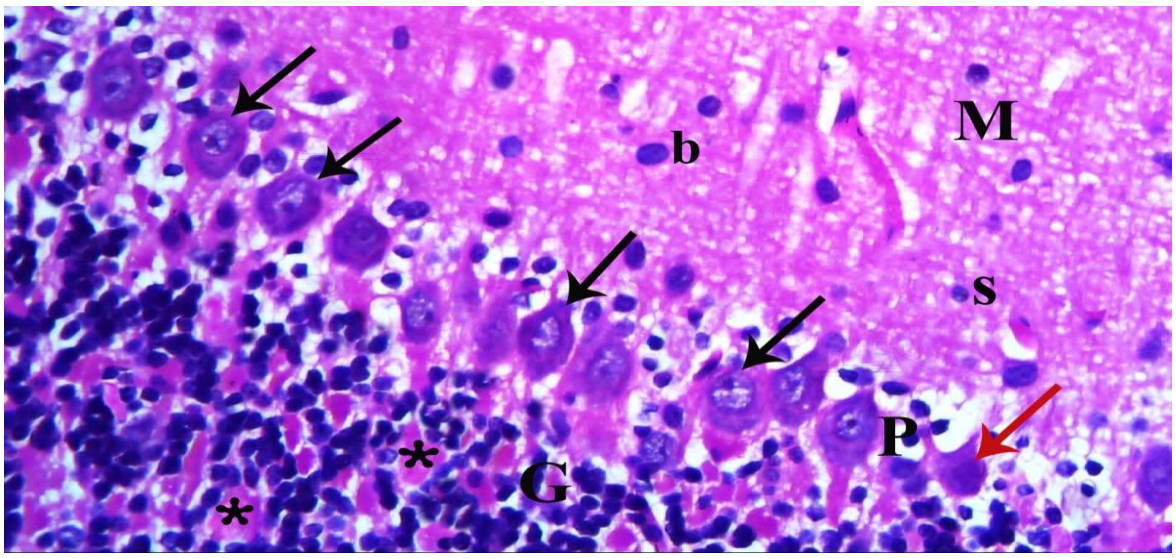

Fig. (6): An H&E-stained photomicrograph of cerebellar segment (**X400**) from group V: viewing apparent normal molecular layer (**M**) comprising stellate cell (**s**) and basket cell (**b**). Single row of pyriform shaped purkinje (**P**) cells (**black arrows**). Only few cells still have pyknotic nucleus (**red arrow**). Closely packed granule (**G**) cells and the cerebellar islands (*).

Immunohistochemical findings

GFAP immune-stained sections from group I and group V displayed positive GFAP immune reaction in some astrocytes. In contrast, group II showed strong immunological expression in the astrocyte processes and soma. Both group III and group IV showed moderate immune reactivity in the astroglial cells (Figure 7A-E).

Caspase-3 immune-stained sections from group I presented negative caspase-3 immune reaction. In contrast, the majority of cells in group II had strong caspase-3 expression in their cytoplasm. Group III and group IV presented less noticeable immune expression of caspase-3.While, Group V presented weak caspase-3 immune reactivity in few cells of the cerebellar cortex (Figures 8A-E).

Cerebellar slices stained with Calbindin from group I displayed strong positive immune reaction to Calbindin protein in numerous Purkinje cells. Group II exhibited reduced immune-reactivity to Calbindin protein. Group III and group IV demonstrated moderate immune expression for calbindin protein in Purkinje cells. However, group V presented intense positive immune reaction in several Purkinje cells (Figures 9A-E).

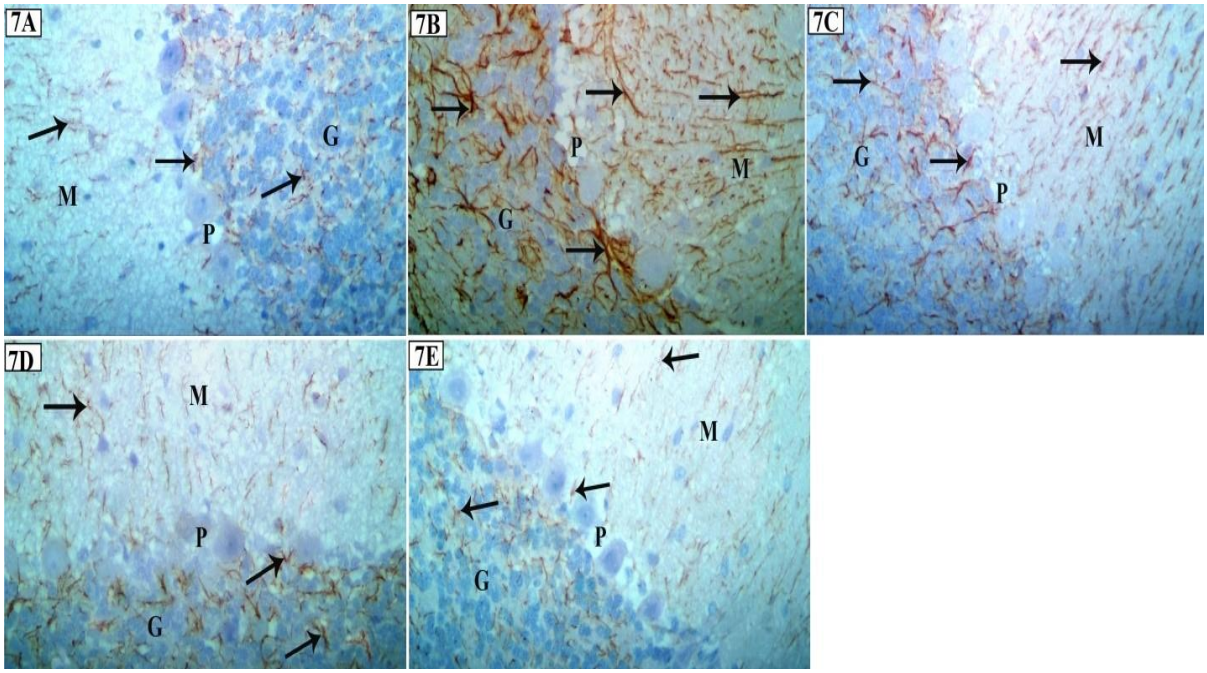

Fig. (7): Photomicrographs of cerebellar tissue presenting molecular layer (**M**), Purkinje cell layer P, granular layer G. Group I 7A & group V 7E showing positive GFAP immune reaction in some astrocytes that appeared faintly brownish (**arrows**) among the different cerebellar cortex layers, Group II 7B displaying intense GFAP immunological response in the soma and many astrocyte processes (**arrows**), group III 7C & group IV 7D showing moderate expression of GFAP (**arrows**) (**GFAP immunostaining x400**).

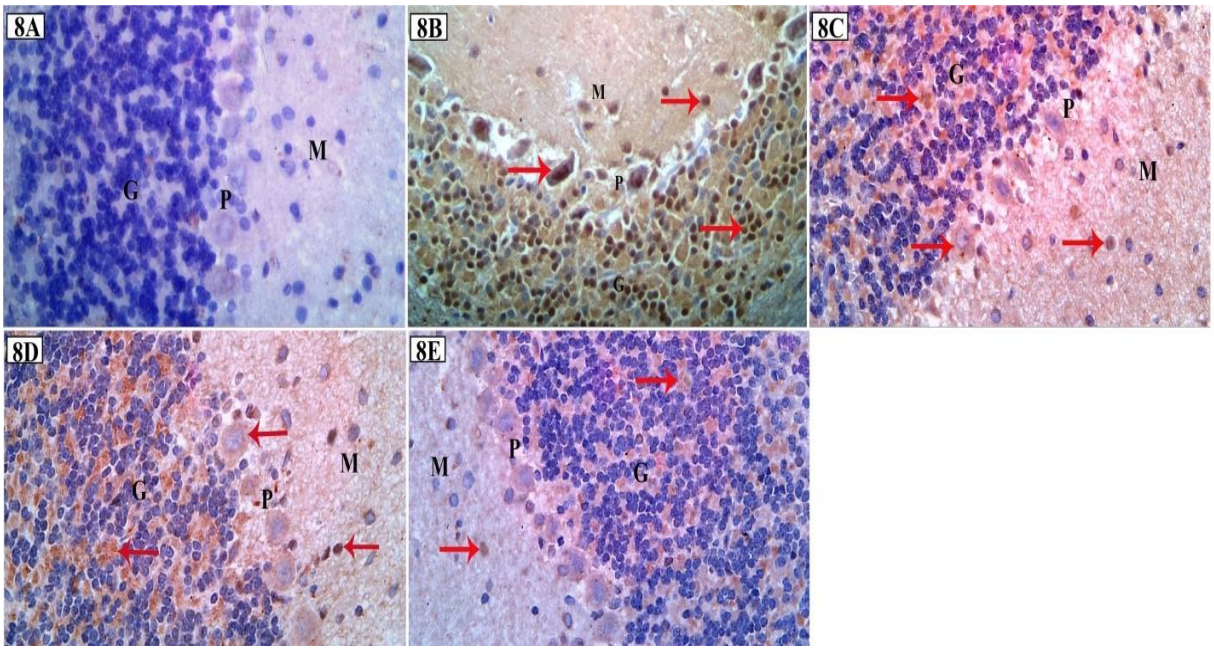

Fig. (8): Photomicrographs from the rat's cerebellar cortex stained with caspase-3 (**X400**); **8A**: Group I presenting negative immunological response to caspase-3 in every layer of the cerebellar cortex, **8B**: Group II presenting powerful caspase-3 immune expression in majority of cells (**red arrows**), Group III **8C** and group IV **8D** presenting less noticeable cytoplasmic immune reactivity for caspase-3 (**red arrows**), **8E**: Group V presenting weak caspase-3 immune reactivity in few cells (**red arrows**).

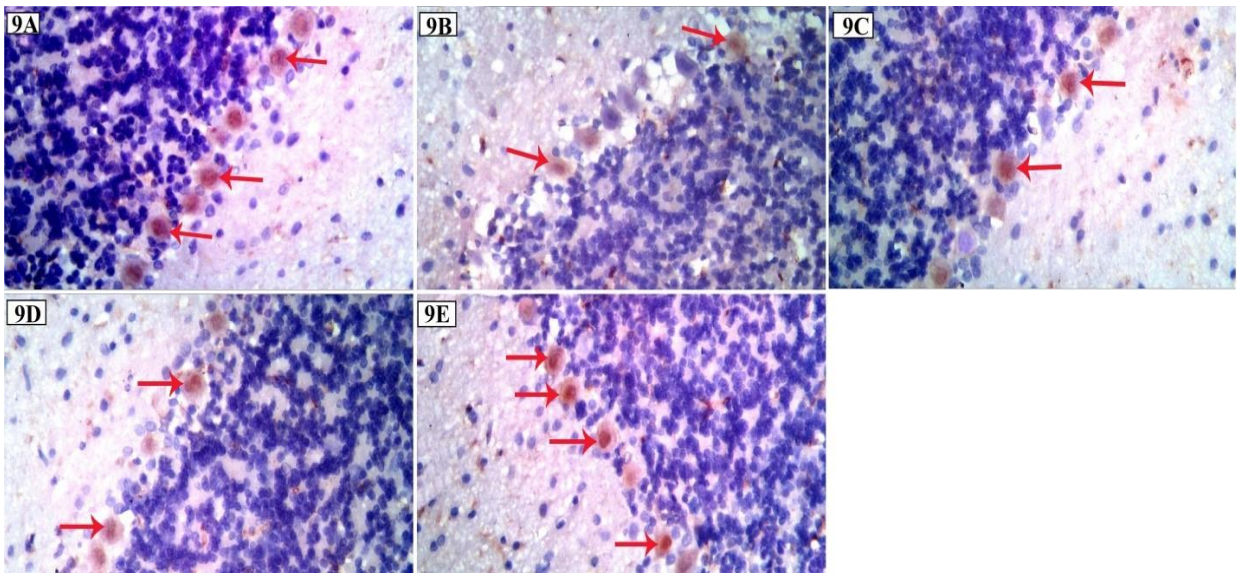

Fig. (9): Cerebellar slices stained with Calbindin immunohistochemical stain (**X400**); **9A**: Group I displaying strong positive immune reaction to Calbindin protein in numerous Purkinje cells (**red arrows**), **9B**: Group II exhibiting reduced immunoreactivity to Calbindin protein (**red arrows**), Group III **9C** and group IV **9D** demonstrating moderate immune expression for calbindin protein (**red arrows**), **9E**: Group V presenting intense positive immune reaction to Calbindin protein (**red arrows**).

Morphometric and statistical results

The mean Purkinje cell number was considerably lower ($P \leq 0.05$) in group II than in group I. Both group III as well as group IV exhibited substantial increase in this number than group II ($P \leq 0.05$) with non-significant variation amongst group III and group IV. About group V, the average number was considerably higher than groups II, III, and IV. However, it was non-significantly differ from group I (Table 2).

Regarding the average area percent of GFAP immune-expression, group II revealed significantly greater value ($P \leq 0.05$) than group I. While, group III as well as group IV displayed momentous decline in the average area percent in relation to group II. In group V, it was considerably lower than group II, III and IV ($P \leq 0.05$) Table 3).

Caspase-3-positive cells' optical density in group II presented markedly higher ($P \leq 0.05$) statistics than group I. Whereas, group III as well as group IV exhibited considerably lower statistics ($P \leq 0.05$) than group II, with non-significant variance ($P > 0.05$) between group III and group IV. However, group V presented a major reduction in these statistics compared to groups II (Table 3).

The calbindin positive cells' optical density was noticeably reduced in group II ($P \leq 0.05$) in relation to group I. Group III as well as group IV exhibited considerably higher results ($P \leq 0.05$) than group II. While, group V displayed highly significant difference ($P \leq 0.05$) compared to groups II, III, and IV but non-significant difference ($P > 0.05$) compared to group I (Table 3).

Table (2): The mean Purkinje cells number among the studied groups (Mean ± SD)

	Group I (n=10)	Group II (n=10)	Group III (n=10)	Group IV (n=10)	Group V (n=10)	P value
Number of Purkinje Cells	12.1 ±0.27	7.1 ± 0.28	10.1 ± 0.21	10.0 ± 0.21	11.9 ± 0.08	<0.001*
Post-hoc	II,III,IV	I,III,IV,V	I,II,V	I,II,V	II,III,IV	

*: significant as P value ≤ 0.05, n: number, SD: standard deviation

Table (3): Area percentage of GFAP immuno-reactivity, caspase-3 optical density and calbindin optical density (Mean ± SD)

	Group I (n=10)	Group II (n=10)	Group III (n=10)	Group IV (n=10)	Group V (n=10)	P value
GFAP immuno-reactivity (%)	16.8 ±0.43	38.7 ± 1.03	24.9 ± 0.72	23.5 ± 0.37	18.1 ± 0.19	<0.001*
Post-hoc	II,III,IV,V	I,III,IV,V	I,II,IV,V	I,II,III,V	I,II,III,IV	
Optical density of caspase-3	0.17 ±0.01	0.54 ± 0.02	0.35 ± 0.02	0.36 ± 0.01	0.23 ± 0.02	<0.001*
Post-hoc	II,III,IV,V	I,III,IV,V	I,II,V	I,II,V	I,II,III,IV	
Optical density of calbindin	0.77 ±0.08	0.23 ± 0.04	0.56 ± 0.02	0.58 ± 0.02	0.74 ± 0.04	<0.001*
Post-hoc	II,III,IV	I,III,IV,V	I,II,V	I,II,V	II,III,IV	

*: significant as P value ≤ 0.05, GFAP: glial fibrillary acidic protein, n: number, SD: standard deviation

Discussion:

ZnONPs have attracted a lot of attention because of their quickly expanding uses in a variety of sectors, such as Nano medicine. Despite their widespread use, the risks associated with their exposure are still unknown (Abass et al., 2017).

The current investigation directed to assess the neurological influence of ZnONPs on the cerebellum of rats and the potential shielding role of selenium and fucoidan.

Our results showed that administration of ZnONPs causes neurodegenerative modifications in the cerebellum of rats. When matched to Group I, Group II revealed a noticeable rise in the tissue MDA levels and a corresponding drop in tissue GSH and SOD. Analogous effects were obtained by Tian et al. 2015 conveyed that exposure to ZnONPs markedly reduced the concentrations of SOD and raised the MDA concentration in the brain of ZnONPs-treated mice.

Additionally, Attia et al. (2018) found that the neurotoxic action technique of

ZnONPs is known to include reductions in GSH, SOD, and catalase (CAT) and increase in proinflammatory cytokines.

On the other hand, this work revealed that the cerebellar tissues of groups III and IV showed a large rise in GSH and SOD levels and a noteworthy drop in MDA levels. It is fascinating to note that combined use of selenium and fucoidan to ZnONPs treated rats in group V significantly brought all of the changed parameters back to levels that were close to those of group I. Consistent with our study, Yang et al. 2022 described the biochemical neuroprotective effects of selenium as GSH levels rose close to normal and decrease MDA level.

Selenium exerts neuroprotective effects by balancing the activities of antioxidants and oxidants (Senol et al., 2014). It also inhibits the pro-inflammatory cytokine interleukin-1β and raises the intensities of the anti-inflammatory cytokine interleukin-4.

Our outcomes in covenant with Wang et al. (2016) who found that fucoidan administration significantly decreased oxidative stress, as evidenced by declined levels of MDA and ROS, as well as inverted activity of glutathione peroxidase and Catalase.

In the existing experiment, H&E-stained sectors from Group II demonstrated numerous pericellular halos and vacuolated neuropils. Purkinje cells were distorted with pyknotic nuclei. These findings were in line with Garman who indicated that vacuolated neuropils may be the consequence of Purkinje cell shrinkage and degeneration, as well as the retraction of their processes, creating empty gaps (Garman, 2011).

In this work, the histological construction of the cerebellar cortex improved in groups III and IV. However, some of Purkinje cells still irregular in shape and had pyknotic nuclei but Group V showed a reasonably normal cerebellar tissue structure. This is reinforced by the work of Tu et al. (2021) who informed that selenium treatment significantly enhanced the cerebellum's architecture in rats. Solovyev (2015) reported that selenium shields the brain against inflammation, endoplasmic reticulum stress, and oxidative damage.

Fucoidan can lessen dopamine neuron cell death and mitochondrial malfunction brought on by toxins. Moreover, it can inhibit microglial activation and lowering the oxidative stress levels which are the main protective effects (Kim et al., 2019).

According to the current study's immunohistochemical analysis of GFAP, exposure to ZnONPs in group II displayed intense immune appearance in the astrocytes. These results are compatible with the outcomes of Abdelrahman et al. (2023) who described significant upsurge in GFAP immunoreactivity in ZnONPs treated animals. Increased astrocyte activation was thought to be a reliable marker for reactive gliosis, which is brought on by injury to the brain's tissue. This could mean that astrocytes could shield and maintain neurons (Liu and Chopp 2016).

This study showed that there was a moderate GFAP immune expression in group III and group IV, while group V displayed positive GFAP immune reaction in few astrocytes. (Salma et al., 2021) also revealed that the combined administration of selenium and ZnONPs greatly enhanced and bring back GFAP expression near the standard status. This indicates that astrocytes sustaining nearby neurons.

Other researchers also noted that nano selenium dramatically decreased GFAP expression, suggesting that nano selenium could mitigate cyclophsphamide-induced neuronal injury and the related astrogliosis (Ibrahim et al., 2021).

The immunohistochemical analysis of caspase-3 in this work revealed that group II had robust immunological expression of caspase-3. This goes in agreement with Khan et al. (2015) and Song et al. (2022) revealed that ZnONPs injection dramatically amplified the zone percentage of the caspase-3 response which is a symptom of apoptosis.

The existing study exposed that the immunological expression of caspase-3 was less evident in groups III and IV and group V. These outcomes are in harmony with Gao et al. (2012) and Huang et al. (2017) which demonstrated that fucoidan reduced apoptosis and shield cells from the stimulation of caspase 3.

Ibrahim et al. (2021) found that in rats cured with both cyclophosphamide and nanoselenium.

There were decrease in the apoptotic index and the area ratio of the caspase 3 response.

A calcium-binding protein called calbindin D28k aids in preserving calcium equilibrium. It stops neuronal death by obstructive a number of pro-apoptotic conduits (Kook et al., 2014).

In our research, Calbindin immunohistochemical staining revealed that animals exposed to ZnONps alone had considerable decreased immunoreactivity to the Calbindin protein. Similar results achieved by Abdelrahman et al. (2023) who mentioned that ZnONP exposure decreased Purkinje cells' calbindin immunoexpression strength. When calbindin is exhausted, neurons' capacity to buffer information is diminished, which causes intracellular and intranuclear calcium levels to rise.

The present experiment showed increased immune expression of calbindin protein in Purkinje cells in groups III, IV and V.

Wirth et al. (2014) described that selenoproteins are precisely needed in post mitotic neurons of the growing cerebellum, and also reported that Purkinje cell staining with calbindin-antibodies revealed a substantial loss of Purkinje cells in the majority of folia in the Cerebellum of mice that lacking selenoproteins. Tu et al. (2021) found that Supplementation with selenium can shield neurons contrary to methylmercury toxicity in the mammalian brain, particularly within the growing cerebellum.

Conclusion:

Numerous detrimental changes in the cerebellar cortex's histological structure were brought on by exposure to ZnONPs. Additionally, these NPs prompted alterations in the oxidative stress indicators, increased GFAP and caspase-3 immune expression suggesting the presence of neurotoxicity. When selenium and fucoidan were administered alone or in combination, these alterations were reversed.

Recommendation

It is recommended to have additional investigations for the effect of different doses of ZnONPs on other human organs.

Conflicts of interest:

Authors have declared that no conflict of interest exists.

References

Abass, M.A., Selim, S.A., Selim, A.O., et al. (2017). 'Effect of orally administered zinc oxide nanoparticles on albino rat thymus and spleen'. *IUBMB life*, 69(7), pp. 528-539.

Abdelrahman, S.A., El-Shal, A.S., Abdelrahman, A.A., et al. (2023). 'Neuroprotective effects of quercetin on the cerebellum of zinc oxide nanoparticles (ZnONPs)-exposed rats'. *Tissue Barriers*, 11(3), pp. 2115273.

Attia, H., Nounou, H. and Shalaby, M. (2018). 'Zinc oxide nanoparticles induced oxidative DNA damage, inflammation and apoptosis in rat's brain after oral exposure'. *Toxics*, 6, p.p. 29.

Bekheet, E. (2020). 'The possible protective role of selenium against long-term phenytoin administration effects on cerebellar cortex of adult male albino rats: Histological and immune-histochemical study'. *Egyptian Journal of Histology*, 43(2), pp. 509-518.

Beutler, E., Duron, O., Kelly, B.M. (1963). 'Improved method for the determination of blood glutathione'. *J Lab Clin Med*., 61, pp. 882–888.

Bi, S.S., Talukder, M., Jin, H.T., et al. (2022). 'Nano-selenium alleviates cadmium -induced cerebellar injury by activating metal regulatory transcription factor 1 mediated metal response'. *Animal Nutrition*, 11, pp. 402-412.

Che, N., Ma, Y., Xin, Y. (2017). 'Protective role of fucoidan in cerebellar ischemia-reperfusion injury through inhibition of MAPK signaling pathway'. *Biomol Ther (Seoul)*, 25(3), pp. 272-278.

Gao, Y., Li, C., Yin, J., et al. (2012). 'Fucoidan, a sulfated polysaccharide from brown algae, improves cognitive impairment induced by infusion of A peptide in rats'. *Environ. Toxicol. Pharmacol*, 33, pp. 304–311.

Garman, R.H. (2011). 'Histology of the central nervous system'. *Toxicol Pathol*, 39(1):pp. 22–35.

Huang, C.Y., Kuo, C.H., Chen, P.W. (2017). 'Compressional puffing pretreatment enhances neuroprotective effects of fucoidans from the brown seaweed sargassum hemiphyllum on 6 -Hydroxydopamine - induced apoptosis in SH-SY5Y cells'. *Molecules*, 23(1), pp. 78

Ibrahim, H.M., Zommara, M.A., Elnaggar, M.E. (2021). 'Ameliorating effect of selenium nanoparticles on cyclo-phosphamide -induced hippocampal neurotoxicity in male rats: light, electron microscopic and immune-histochemical study'. *Folia Morphol (Warsz)*, 80(4), pp. 806-819.

Ibrahim, R.K., Hayyan, M., AlSaadi, MA., et al. (2016). 'Environmental application of nanotechnology: air, soil, and water'. *Environ. Sci. Pollut. Res.*, 23(14), pp. 13754–13788.

Khan, S., Ahmad, K., Alshammari, E.M.A., et al. (2015). 'Implication of caspase-3 as a common therapeutic target for multi-neuro-degenerative disorders and its inhibition using nonpeptidyl natural compounds'. *Bio Med Research International*, pp. 1-9.

Kiernan, J.A. (2015). Histological and Histochemical Methods: Theory and Practice, 5th edition, Scion Publishing Ltd, Banbury, UK, pp. 571.

Kim, H., J. H., Ahn, M., et al. (2019). 'Park pretreated fucoidan confers neuro-

protection against transient global cerebellar ischemic injury in the gerbil hippocampal CA1 area via reducing of glial cell activation and oxidative stress'. *Biomedicine & Pharmaco-therapy*, 109, pp.1718-1727.

Kook, S.Y., Jeong, H., Kang, M.J., et al. (2014). 'Crucial role of calbindin-D 28k in the pathogenesis of Alzheimer's disease mouse model'. *Cell Death Differ*, 21(10), pp. 1575–1587.

Liu, Z. and Chopp, M. (2016). 'Astrocytes, therapeutic targets for neuroprotection and neurorestoration in ischemic stroke'. *Prog Neurobiol*, 144, pp. 103–120.

Nishikimi, M., Rao, N.A. and Yagi, K. (1972). 'The occurrence of superoxide anion in the reaction of reduced phenazine methosulfate and molecular oxygen'. *Biochem Biophys Res Commun*, 46(2), pp. 849–854.

Ohkawa, H., Ohishi, N. and Yagi, K. (1979). 'Assay for lipid peroxides in animal tissues by thiobarbituric acid reaction'. *Anal Biochem*; 95(2), pp.351–358.

Ramos-Vara, J.A., Kiupel, M., Baszler, T., et al. (2008). 'Suggested guidelines for immune-histochemical techniques in veterinary diagnostic laboratories'. *J Vet Diagn Investig*, 20(4), pp. 393–413.

Salma, S.N., El-Sayed, N.S. and Abd El-Gawad, I.M. (2021). 'Selenium protects caspase 3 and glial fibrillar acidic protein (GFAP) expression in cerebellum of rats against zinc oxid nanoparticles (Znonps) exposure'. *Annals of the Romanian Society for Cell Biology*; 25(6), pp. 08-23.

Senol, N., Nazıroglu, M. and Yuruker, V. (2014). 'N-acetylcysteine and selenium modulate oxidative stress, antioxidant vitamin and cytokine values in traumatic brain injury-induced rats'. *Neurochemical Research*, 39, pp. 685-692.

Solovyev, N.D. (2015). 'Importance of selenium and selenoprotein for brain function: from antioxidant protection to neuronal signaling'. *J. Inorg. Biochem*, 153, pp. 1–12.

Somayeh, B. and Mohammad, F. (2014). 'Vitamin C can reduce toxic effects of Nano Zinc Oxide'. *Int J Biological Sci*, 3, pp. 65–70.

Song, W.J., Kim, J., Shin, T., et al. (2022). 'Esculetin and Fucoidan attenuate autophagy and apoptosis induced by zinc oxide nanoparticles through modulating reactive astrocyte and proinflammatory cytokines in the rat brain'. *Toxics*, 10(4), pp. 194.

Tian, L., Lin, B., Wu, L., et al. (2015). 'Neurotoxicity induced by zinc oxide nanoparticles: age-related differences and interaction'. *Sci Rep*, 5, pp. 16117.

Torabi, F., Shafaroudi, M.M. and Rezaei, N. (2017). 'Combined protective effect of zinc oxide nanoparticles and melatonin on cyclophosphamide-induced toxicity in testicular histology and sperm parameters in adult Wistar rats'. *Int J Reprod Biomed*, 15(7), pp. 403-412

Tu, R., Zhang, C., Feng, L., et al. (2021). 'Impact of selenium on cerebellar injury and mRNA expression in offspring of rat exposed to methyl mercury'. *Ecotoxicology and Environmental Safety*, 223, pp. 112584.

Wang, T., Zhu, M. and He, Z.Z. (2016). 'Low –molecular -weight fucoidan attenuates mitochondrial dysfunction and improves neurological outcome after traumatic brain injury in aged

mice: Involvement of Sirt3'. *Cell Mol. Neurobiol*, 36, pp. 1257–1268.

Wang, Y., Wang, Q., Han, X., et al. (2021). 'Fucoidan: A promising agent for brain injury and neurodegenerative disease intervention'. *Food Funct.*, 12, pp. 3820–3830.

Wirth, E.K., Bharathi, B.S., Hatfield, D., et al. (2014). 'Cerebellar hypoplasia in mice lacking selenoprotein biosynthesis in neurons'. *Biological Trace Element Research*, 158, pp. 203-210.

Yang, J.Y., Du, J.J., Zhang, Y.F., et al. (2022). 'Vitamin E and selenium partially prevent cytotoxicity, oxidative stress and DNA damage induced by T-2 toxin in bovine Leydig cells'. *Theriogenology*, 189, pp. 255-261.

Zhang, C., Ge, J., Lv, M., et al. (2020). 'Selenium prevent cadmium-induced hepatotoxicity through modulation of endoplasmic reticulum -resident selenoproteins and attenuation of endoplasmic reticulum stress'. *Environmental Pollution* 2020, 260, pp. 113873.

تأثير الجسيمات النانوية لأكسيد الزنك على المخيخ في ذكور الجرذان البيضاء البالغة والدور الوقائي المحتمل للسيلينيوم والفوكويدان (دراسة نسيجية ومناعية كيميائية)

أمال غنيمي متولي فرج[1], أميمة رفعت محمد[2], أمينة محمد نجاح محمد اسماعيل[3], نهال فهمي شاهين[4]

[1] مدرس بقسم التشريح والاجنة بكلية الطب جامعة بنها

[2] مدرس بقسم الطب الشرعي والسموم الاكلينيكية بكلية الطب جامعة بنها

[3] مدرس بقسم الامراض العصبية والطب النفسي بكلية الطب جامعة بنها

[4] استاذ مساعد بقسم التشريح والاجنة بكلية الطب جامعة بنها

لقد حظيت الجسيمات النانوية لأكسيد الزنك بالكثير من الاهتمام بسبب استخداماتها المتزايده في العديد من الصناعات.

هدفت هذه الدراسة الي تقييم تأثير الجسيمات النانوية لأكسيد الزنك على أنسجة المخيخ للفئران والوظيفة الوقائية العصبية المحتملة للفوكويدان والسيلينيوم.

تم فصل خمسين من الفئران البيضاء البالغة إلى خمس مجموعات؛ المجموعة الأولى (الضابطة)، المجموعة الثانية أعطيت 400 ملجم/كجم من وزن الجسم من الجسيمات النانوية لأكسيد الزنك داخل الصفاق لمدة شهر واحد، تم إعطاء المجموعة الثالثة الجسيمات النانوية لأكسيد الزنك بالإضافة إلى السيلينيوم عن طريق الفم بجرعة 0.5 ملجم / كجم من وزن الجسم / يوم لمدة شهر واحد، تم حقن المجموعة الرابعة بالجسيمات النانوية لأكسيد الزنك بالإضافة إلى حقن الفوكويدان داخل الصفاق بجرعة يومية. من 80 ملجم / كجم من وزن الجسم لمدة شهر واحد وتم حقن المجموعة الخامسة بالجسيمات النانوية لأكسيد الزنك بالإضافة إلى السيلينيوم و فوكويدان لمدة شهر واحد. تم تحضير عينات القشرة المخيخية لإجراء الفحوصات النسيجية والكيميائية الحيوية والمناعية. وأجريت التقييمات باستخدام كل من الأساليب المورفومترية والإحصائية.

قامت الجسيمات النانوية لأكسيد الزنك برفع مستويات MDA بشكل ملحوظ، في حين خفضت بشكل ملحوظ مستويات SOD وGSH مقارنة بالمجموعة الضابطة. من الناحية النسيجية، تم تدمير خلايا بوركنجي. في حين أن متوسط مساحة المنطقة المناعية لـ GFAP والخلايا الإيجابية لكاسبيز 3 زادت بشكل كبير، فإن الكثافة البصرية للخلايا المناعية للكالبيندين انخفضت بشكل كبير. بالمقارنة مع مجموعة الجسيمات النانوية لأكسيد الزنك ، خفضت علاجات السيلينيوم والفوكويدان بشكل كبير مستويات MDA وحسنت بشكل كبير مستويات SOD وGSH، وحسنت البنية المخيخية النسيجية، وانخفضت الصبغة المناعية للخلايا الإيجابية لـ GFAP وcaspase-3 بشكل ملحوظ بينما زادت الخلايا المناعية للكالبيندين.

أدى تناول السيلينيوم والفوكويدان إلى تحسين التغيرات المخيخية الناجمة عن الجسيمات النانوية لأكسيد الزنك بشكل كبير في الفئران.